Hydrogen Effects on Tensile Property of Pure Iron with Deformed Surface

Shuai Wang[a, 1], Somei Ohnuki[a], Naoyuki Hashimoto[a], Keisuke Chiba[a]

[a] Department of Materials Science and Engineering, Hokkaido University, N13 W8, Kita-ku, Sapporo Hokkaido, 060-8628, Japan

Abstract

To study the interaction of hydrogen and surface structure of iron, two types of tensile test are carried out under hydrogen gas environment and cathodic hydrogen charging condition. According to the tensile tests, hydrogen induces reduction of flow stress (softening) for the specimens without deformed surface, but increase of flow stress (hardening) for the one with deformed surface. The results of jump tests signify that hydrogen enhances the dislocation mobility by reducing the thermal activation volume for overcoming barriers, and because of this, in the samples with smooth surface, homogeneously distributed hydrogen leads to the softening effect. On the other hand, the deformed layer just under the surface has larger solubility of H due to trap sites provided by dislocation cell structures. As a result of hydrogen shielding effect, the strong interaction between dislocations in surface layer and multiplication of new defects causes the hardening effect.

Keywords: Hydrogen; Surface; Deformation; Dislocation structure

[1] Corresponding author. TEL: +81-11-706-6772, FAX: +81-11-706-6769.
E-mail address: towangshuai@eng.hokudai.ac.jp

1. Introduction

Over the past 50 years, many research works have been dedicated in order to find out the effect of hydrogen on mechanical properties of ferrite-based alloy, although arguments still exist in nowadays [1-3]. The degradation of mechanical properties of metal under hydrogen atmosphere is termed as hydrogen embrittlement (HE) and it has been well explained by the theory of hydrogen enhanced local plasticity (HELP) [3], which becomes one of the most acceptable mechanisms in the studies focusing on the HE issues. TEM in-situ observation on a number of metals has shown the velocity of dislocation is improved in a hydrogen gas environment cell [4]. There are also reports that have provided direct evidences for formation of new dislocation slip plane and nucleation of equilibrium vacancies caused by hydrogen [5, 6]. Some calculation works indicate that hydrogen solutes can influence dislocation motion by weaken stress field between dislocation and barrier, which is termed as hydrogen induced shielding effect (or screening effect) [7, 8].

However, in some metals, whether hydrogen induces softening (decrease of flow stress) or hardening (increase of flow stress) effect, for example pure iron [9] and also Ni, Al [10, 11], is still a puzzle. Matsui and Kimura [9, 11] have suggested that the variety of results is attributable to irreversible damage induced by the cathodic charging process, and in high purity iron the hydrogen effect was observed either as softening or hardening depending on the temperature. In practical application, the influence of surface structure is an important issue for the hydrogen storage material and also the structure material utilizing under hydrogen atmosphere. Fidelle et. al reported that [12], by comparing the disk pressure tests for 35NCD16HS steel with different surface conditions, the one with smoother surface can sustain larger stress under high hydrogen

pressure, and the rough surface of container is believed to be dangerous for storage of hydrogen. Additionally, many articles have emphasized the importance of surface condition for hydrogen charging tensile test [13, 14]. However, there is limited discussion focusing on the influence of deformed surface on mechanical properties of hydrogen charged specimen.

The interaction of manually introduced deformed surface layer and hydrogen will be discussed in this paper using tensile tests under high-pressure hydrogen gas environment (hydrogen gas tensile tests) and simultaneous hydrogen charging condition (dynamic hydrogen charging tensile tests). The results here would enable an understanding of details for the influence of hydrogen on mechanic properties of pure iron with deformed surface.

2. Experimental

Two experimental methods were carried out in this study: hydrogen gas tensile tests with rod specimens and dynamic hydrogen charging tensile tests with small size plate specimens. As an ordinary tensile test, hydrogen gas tensile test demonstrates the variation of tensile properties influenced by hydrogen and deformed surface. Dynamic hydrogen charging tensile test is one kind of small specimen test techniques, which is helpful for obtaining homogeneously distributed hydrogen and details for dislocation behavior with hydrogen.

2.1 Hydrogen gas tensile test

Pure iron with purity better than 99.96% was used for fabricating tensile specimens and the chemical compositions is shown in Table 1. The tensile rods have dimensions as illustrated in Fig. 1, and they were subjected to Instron tensile machine with a constant strain rate of $6.7\times10^{-4}\ s^{-1}$, at 293 K under 30 MPa hydrogen gas environments (purity of

hydrogen is 99.99999%). The tensile test was started immediately as the sample subjected into hydrogen atmosphere and the test was finished within 15 minutes. As shown in Fig. 1, two surface conditions were introduced: one had the surface as lathed and the other had polished surface by buffering (marked as polished sample). The surface of the polished sample is smoother than the lathed specimen and the deformed layer is about 5 □m thinner. The hydrogen free rods were also tested for comparison. After tensile test, the specimens were investigated by scanning electron microscope (SEM, JEOL JEM-6500F).

2.2 Dynamic hydrogen charging tensile test

Pure iron used in this section has the same purity as in hydrogen gas tensile test. The raw materials were cold rolled to 0.3 mm plates and small size specimens have dimensions as shown in Fig. 2. Since hydrogen has a high diffusion constant in pure iron (at 293 K, D=7.0×10^{-9} m^2/s [15]), hydrogen atoms can transfer quickly in the specimens. For a lattice diffusion controlling process, the diffusing thickness L can be estimated as a function of time [21]: $L = \sqrt{6Dt}$, from which one can find that within 5 s the hydrogen atoms can diffuse though a distance of 0.46 mm and it is longer than the thickness of small size specimens applied in this experiment. The hydrogen concentrations mainly depend on the microstructures, in particular the dislocations and other defects that provide large amounts of trap sites for hydrogen.

The small plates were enveloped into vacuum quartz tube and then annealed at 1027K for 30 min. Four kinds of surface condition were obtained after annealing: (1) specimens after electrochemical polishing using an electrolyte of Acetic acid: Perchloric acid=19: 1 (marked as EP samples), which have the thinnest deformed surface; (2) specimens as annealed, without further polishing; (3) specimens grinded on Struers

water-proof SiC abrasive paper, with grit #1000 (marked as #1000 samples); (4) specimens grinded on abrasive paper with grit #100 (marked as #100 samples) which have the thickest deformed surface layer. All the samples were tested for at least three times and average values for characterizing tensile properties were obtained.

The stress distribution in the deformed surface was investigated by the electron backscatter diffraction (EBSD) technology. TEM (JEM-2010) was used to observe the surface microstructure of #100 samples. The foils for TEM observation were prepared by ion slice method using JOEL Ion Slicer (EM-09100IS).

The tensile experiments were carried out on an Instron 5564 universal tensile test machine at 293 K with a constant strain rate of 6.7×10^{-4} s^{-1}. The electrolyte for the cathodic charging was 0.5 mol/l H_2SO_4. Hydrogen charging using a potentiostat/galvanostat (Hokuto HA151, galvanostat mode) was performed during the tensile tests. It has been reported that high current density may cause high fugacity hydrogen in the interface and produce irreversible damage by which any intrinsic effect of hydrogen could be masked in subsequent tests [16], thus low cathodic current density of 7 mA/cm^2 was used to prevent such damage on sample surface. In order to make sure that the gauge area of tensile specimen was mainly charged, micro-shield painting was applied on the top of the specimens. The cathodic charging was continued all though the tensile test and the total charging time was around 10 minutes. SEM was applied to investigate the morphology of surface and fracture after tensile tests.

The activation volume measured by jump test (changing the strain rate during tensile test) gives information of thermally activated behavior for dislocations overcome short-range obstacles (forest dislocations, vacancies and energy barrier for cross-slip of dislocations, etc.) and also the mobility of dislocations [17]. Jump tests in this study

were taken by varying the strain rate from 1.0×10^{-4} s^{-1} to 1.0×10^{-2} s^{-1} and three temperatures (273K, 283K, and 293K) were chosen to investigate the influence of H concentration on hydrogen-dislocation interactions.

3. Results

3.1 Tensile tests under hydrogen gas atmosphere

3.1.1 Hydrogen concentrations of rod specimens

The hydrogen concentration in rod specimens can be estimated following an equation established by Gonzalez [18]:

$$C(appm) = 2.35 P_H \exp(-\frac{6500}{RT}) \quad (1)$$

in which P_H is the pressure of hydrogen gas in unit of atm and R is the gas constant (8.31 $J\cdot mol^{-1}K^{-1}$). As P_H = 30 MPa (300 atm) in this experiment, at 293 K the hydrogen concentration in the rod specimen without deformed surface is about 2.82 appm. However, the dislocations in deformed surface have ability to trap more hydrogen and increase local hydrogen concentration near surface. Since the as-lathed sample has thicker deformed layer near surface, local hydrogen concentration in the deformed layer is higher compared with the polished one.

3.1.2 Variation of tensile properties for rod specimens

The results of tensile tests obtained in hydrogen atmosphere are shown in Table 2, and the variations of yield stress (YS), ultimate tensile stress (UTS) and elongation after introducing hydrogen are calculated as Δ (H-Air). With hydrogen, the YS and UTS of polished specimen decrease a lot, and the elongation increases. On the other hand, the elongation for lathed sample decreases, and the decrease of YS and UTS are less than the polished one. From the surface and fracture topographies shown in Table 3, the crack mode in rod specimens changes from a cup-cone fracture in air to a slant facture

in hydrogen gas and the percentage reduction of area (%RA) is decreased. There is less ductile area on the fracture in hydrogen gas, and lots of micro-cracks are found on the lathed surface but less on the polished one. The %RA of the lathed sample is much lower than the polished one when subjected to H atmosphere, which indicates the sensitivity of hydrogen embrittlement is higher in the lathed sample.

3.2 Tensile tests under hydrogen charging condition

3.2.1 Hydrogen concentration under hydrogen charging condition

By the theory of Oriani, the hydrogen trapped in the matrix mainly depends on the type of trapping site and the trap binding energy [19]:

$$\frac{q_T}{1-q_T}=\frac{q_L}{1-q_L}\exp(\frac{E_B}{RT}) \tag{2}$$

where θ_L denotes the occupancy of the interstitial sites, θ_T denotes the occupancy of the trapping sites, E_B is the trap binding energy (for dislocation in iron, E_B = 30 kJ/mol [19]), and T is absolute temperature. The hydrogen concentration measured in atoms per unit volume in lattice sites and trapping sites are $C_L=\theta_L\beta N_L$ and $C_T=\theta_T\alpha N_T$ respectively. Here β is the number of interstitial sites per solvent atom, α is the number of trapping sites per trap, N_L denotes the number of solvent atoms per unit volume (8.46×10^{28} m^{-3} for Fe), N_T is the trap density. In the model developed by Sofronis et.al [20], by assuming that one hydrogen atom is trapped per atomic plane threaded by a dislocation, trap density for dislocations is $N_T=\sqrt{2}\,\rho/a$, in which ρ is the dislocation density of iron (measured by TEM, for stress free sample $\rho=2\times10^{13}$ m^{-2}) and a is lattice constant.

At certain hydrogen cathodic current i_c, the balance hydrogen concentration in lattice sites can be expressed in the form of Sievert's law, $C_L=Ki_c^{1/2}$. Details of this law have been determined by hydrogen charging permeation tests by Jonson and Wu [21, 22]:

$$C_L = \frac{j_0 N_a}{D_0} \exp\left(\frac{-8000}{RT}\right)\sqrt{i_c} \quad (3)$$

where φ_0 is permeation constant (for pure iron, 3.70×10^{-6} mol·m^{-1}s^{-1} (mA·cm^{-2})$^{-1/2}$ [21]), D_0 is diffusion constant (for pure iron, D_0= 2.1×10^{-7}m^2/s [21]), and N_a is Avogadro constant.

From equations 2 and 3, at T=293 K, the hydrogen trapped in matrix for the sample without deformed surface is about 12.40 appm, and the hydrogen trapped by dislocations in pure iron is about 0.38 appm. The local hydrogen concentration near the deformed surface is calculated as a function of the dislocation density, as shown in Fig. 3. In the #100 sample, by using the dislocation density just under the deformed surface estimated from TEM observation in next section, hydrogen concentration in the deformed surface layer is found to be almost three times more than in the substrate area.

3.2.2 Microstructure of the deformed surface

The stress field of deformed layer is different from the substrate area (the un-deformed area), and which can be displayed by the image quality (IQ) from results of EBSD. The image quality in an EBSD image can be calculated as follows: IQ=intensity of diffraction pattern/ intensity of background.

The results of EBSD obtained from the deformed area of #100 samples are presented in Fig. 4a - Fig. 4d. Compared with the homogeneous distributed color map in the EP sample (in Fig. 4a and 4c), there is a segregation band with a thickness of 4-6 μm in the #100 sample (Fig. 4b and 4d), which signifies region of stress concentration has been manually introduced beneath the surface.

The dislocation arrangement just under the surface of #100 sample was observed by TEM and demonstrated in Fig. 5. Different from the dislocation lines deep into the substrate area, dislocation cells are formed with a thickness around 4-6 μm under the

deformed layer. The shape and position of this deformed structure are in accordance with the stress concentration band observed by EBSD.

3.2.3 Variations of tensile properties of small size specimens

From dynamic hydrogen charging tensile test, the results of YS and UTS are illustrated in Table 4. The YS and UTS for EP sample decreases during H charging, and the elongation increases, which indicate H softening effect. In the case of the as-annealed, #1000 and #100 specimens, imposing hydrogen reduces total elongations. The #100 sample has the lowest elongation but the highest YS and UTS in dynamic hydrogen charging tests. H induces hardening effect in the samples with deformed surface.

From the SEM observation, the typical morphologies of the surfaces and the fracture at different hydrogen charging conditions are summarized in Table 5. The fracture changes from ductile type in the air to partly brittle type with hydrogen, which is in the same rule as observed in the hydrogen gas tensile test. There are lots of micro-cracks on the surface of #100 specimens, but none of the cracks is found on the EP specimens. By hydrogen charging the %RAs of the two small specimens are decreased, and the decreased %RA for #100 sample is larger than the EP sample.

3.2.4 Activation volume measurement

The activation volume of the dislocation motion can be calculated by the following equation [23]:

$$\Delta V = kT \frac{\ln(\dot{\varepsilon}_2 / \dot{\varepsilon}_1)}{\tau_2 - \tau_1} \tag{4}$$

where $(\tau_2 - \tau_1)$ refers to the change in flow stress when stain rate varies from $\dot{\varepsilon}_1$ to $\dot{\varepsilon}_2$, and k is the Boltzmann constant. The activation volume is measured in a unit of b^3, and b is Burgers vector which equals 0.248 nm in the case of BCC iron. The shear stress τ in Eq.

4 is related to the normal stress σ by the Taylor orientation factor. A Taylor factor of 3 for iron is applied in this study: $\tau = \sigma/3$ [24].

The result of thermal activation analysis is shown in Fig. 6. Hydrogen charged specimen has smaller activation volume than the hydrogen free one, which indicates that the dislocations inside the EP sample have a higher mobility than the hydrogen free sample. At 273 K, the hydrogen concentration is the highest due to the diffusion of hydrogen is slower in lower temperature, C_L (273 K)=15.77 appm according to Eq. 3. The activation volume in the sample tested with hydrogen charging at 273 K is lower than the samples tested at higher temperatures of 283 K (C_L (283 K)=13.93 appm according to Eq. 3) and 293 K (12.78 appm), which provides evidence that the increase of dislocation mobility is proportional to the amount of hydrogen trapped in matrix.

4. Discussions

4.1 The correlations between the two types of tensile test

For the hydrogen gas tensile tests, the elongation for the as-lathed sample decreases and the absolute value of ΔYS and ΔUTS are much smaller than the polished one. This might because of that, the deformed layer introduced in the as-lathed sample has much higher ratios in the total thickness compared with the polished one and the hydrogen-enhanced interaction of surface dislocations and other defects could be more severe for as-lathed sample.

For the hydrogen charging tensile tests, typical hydrogen-induced softening effect is found in the specimens without deformed layer. On the contrary, the samples with deformed surface have more micro-cracks, lower %RA and higher flow stresses during plastic deformation that indicate hydrogen induces hardening effect.

Comparing the results from the two types of tensile tests, it is remarkable that the

increasing of defect density in surface layer is the main contributor to the enhanced sensitivity of hydrogen embrittlement.

4.2 The interactions of hydrogen and dislocation

According to the results of EBSD and TEM observation presented before, grinding on abrasive paper introduces dislocation cells with thickness around 5 μm under the surface, which have higher ability for trapping hydrogen than the un-deformed substrate area. In dynamic hydrogen charging tensile test, the hydrogen concentration introduced into the lattice is about 12 appm for the substrate area at 293 K, while in the deformed layer of #100 sample the hydrogen concentration is more than 30 appm.

The critical strain rate ε_c for dislocation to break away from its hydrogen atmosphere is estimated as $\varepsilon_c=\rho_m b v_c$ [25], where ρ_m is the mobile dislocation density and $v_c=4DkT/(E_B r_c)$ (r_c is the dislocation core radius). In the case mobile dislocation density equals 10^{13} m^{-2}, ε_c is calculated to be 1.6×10^{4} s^{-1}. The strain rates used in this study are much lower than this value.

From the simulation work by Sofronis et. al [7], with hydrogen atmosphere the interaction distance between dislocations are expected to decrease. The decrease of activation volume obtained from jump tests in this study is in good agreement with their analysis, and hydrogen can increase the mobility of dislocations in specimens with or without deformed surface according to hydrogen shielding effect.

4.3 The influences of hydrogen on the plastic behavior

For pure iron without deformed surface, there are dislocation lines distributed in the matrix with a low density, as illustrated in Fig. 7a. By hydrogen shielding effect, the mobility of dislocation line is enhanced, and hydrogen can decrease the flow stress by a mechanism of reducing the thermal activation volume for overcoming short-range

obstacles, thus the softening phenomenon can be observed.

By grinding the surface of pure iron on abrasive papers, there are dislocation cell structures introduced in the deformed layer as shown in Fig. 7b. By the same mechanism as in the substrate area, high concentration of hydrogen also encourages the mobility of dislocations in the deformed layer. However, hydrogen with high concentration can enhance the formation of new defects as reported in other research work [5]. For the encouraged strong interaction between dislocations accompanied with multiplication of new defects, higher flow stress is needed for operating the dislocations and the hardening phenomenon can be observed. On the other hand, from the activation volume measurement, the influence of hydrogen shielding effect is proportional to the H concentration. The H concentration gradient from deformed layer to the substrate area gives rise to non-uniform distributed internal stress. The strong interactions of dislocations could encourage initiation of micro-cracks on the surface, and the fracture behavior will happen in the early stage of plastic deformation for iron with deformed surface.

5. Conclusions

By the hydrogen gas atmosphere tensile experiment and dynamic hydrogen charging tensile experiment, the hydrogen effects on tensile property of pure iron with deformed surface are discussed.

1. The tensile tests under hydrogen gas environment and hydrogen charging conditions have shown consistent results that, hydrogen induces softening effect for the pure iron with smooth surface and thin deform layer, but hardening effect when the surface is severely deformed.

2. By grinding on abrasive papers, dislocation cell structures with a thickness of 4-6

μm are formed just under the surface. As the deformed layer provides more trapping sites for hydrogen, local H concentration in surface layer is almost three times more than in the substrate area.

3. Hydrogen can be trapped by slow moving dislocation and influence the plastic behavior by hydrogen shielding effect, however, the consequences of hydrogen shielding effect in the substrate area and the deformed structure are different.

In the substrate area, the dislocation motion is enhanced by a mechanism of decreasing the activation volume for dislocation motion according to hydrogen shielding effect. Only with such dislocation structure in the specimen, hydrogen induces softening effect during plastic deformation.

In the deformed layer, the high value of hydrogen concentration enhances the formation of defects and higher flow stress is needed for operating dislocations and further dislocation motion. Hydrogen induced relaxation of internal stress field is mainly controlled by the H concentration. For the hydrogen concentration in deformed layer is different from the substrate area, a gradient of internal stresses could be introduced during tensile tests. As a result, hydrogen induces hardening effect in the pure iron with deformed surface and also increases probability for forming micro-cracks on the surface.

References

[1] R.A. Oriani, P.H. Josephic, Acta. Metall. 22(1974): 1065-1047.

[2] D.S Shih, I.M Robertson, H.K. Birnbaum, Acta. Metall. 36 (1988): 111-124.

[3] S.M. Myers, M.I. Baskes, H.K. Birnbaum, et. al, Rev. Mod. Phys. 64(1992): 559-617.

[4] P.J. Ferreira, I.M. Robertson, H.K. Birnbaum, Acta. Mater. 46(1998): 1749-1757.

[5] T.D. Lee, I.M. Bernstein, Acta. Metall. Mater. 39(3)(1991): 363-372.

[6] V.G. Gavriljuk, V.N. Bugaev, et. al, Scripta. Mater. 34(6)(1996): 903-907.

[7] P. Sofronis, H.K. Birnbaum, J. Mech. Phys. Solids 43(1)(1995): 49-90.

[8] J.P. Chateau, D. Delafosse, T. Magnin, Acta. Mater. 50(6)(2002): 1507-1522.

[9] H. Matsui, H. Kimura, S. Moriya, Mater. Sci. Eng. 40(1979): 207-216.

[10] J.W. Watson, Y.Z. Shen, M. Meshii, Metall. Trans. A 19A(1988): 2299-2305.

[11] A. Kimura, H.K. Birnbaum, Scripta. Metall. 21 (1987): 53-57.

[12] J.P. Fidelle, ASTM STP 543(1974): 221-253.

[13] D. Tromans, Acta. Metall. Mater. 42(1994): 2043-2049.

[14] S. Modiano, J.A. Carreno, et. al, Electrochim. Acta. 51(2005): 641-648.

[15] H. Hargi, Y. Hayashi, N. Ohtani, Trans. JIM. 20(1979): 349.

[16] I.G. Park, A. Thompson, Metall. Mater. Trans. A 21(1990): 465-477.

[17] D.T. Hoelzer, A.F. Rowcliffe, J. Nucl. Mater. 307-311 (2002): 596-600.

[18] O.D. Gonzalez, Trans. Metall. Soc. AIME. 245 (1969): 607-612.

[19] R.A. Oriani, Acta. Metall. 18(1970): 147-157.

[20] P. Sofronis, Y. Liang, N. Aravas, Eur. J. Mech. A/Solids. 20(2001): 857-872.

[21] D.L. Johnson, J.K. Wu, J. Mater. Energy System 8(1987): 402-408.

[22] J.K. Wu, Int. J. Hydrogen Energy 17 (1992): 917-921.

[23] Y.M. Wang, A.V. Hamza, E. Ma, Appl. Phys. Lett. 86(2005): 241917.

[24] J.M. Rosenberg, H.R. Piehler, Metall. Mater. Trans. B 2(1) (1971): 257-259.

[25] J.K. Tien, A.W. Thompson, I.M. Bernstein, et. al, Metall. Mater. Trans. 7A (1976): 821-829.

Figure legends

Fig. 1 the dimensions of sample for hydrogen gas tensile tests and surface conditions of polished sample and as-lathed one.

Fig. 2 the dimensions of specimen for dynamic hydrogen tensile test.

Fig. 3 the hydrogen concentration in the surface layers calculated as a function of dislocation density.

Fig. 4 the observation of surface structures of EP and #100 samples by SEM: (a) SEM microstructure of EP sample; (b) SEM microstructure of #100 samples; (c) EBSD figure of EP sample; (d) EBSD figure of #100 samples.

Fig. 5 the dislocation structure observed by TEM in the surface area of #100 samples.

Fig. 6 the activation volume of EP samples measured from jump test in different temperature.

Fig. 7 the schematic diagram for possible hydrogen behavior at different surface structures.

Table legends

Table 1 the composition of pure iron used in this study (in wtppm).

Table 2 the variation of tensile properties in rod specimen.

Table 3 the summary of surface topography after tensile test in hydrogen gas environment.

Table 4 the variation of tensile properties in small size specimen.

Table 5 the summary of surface topography after dynamic hydrogen charging tensile test.

Figures

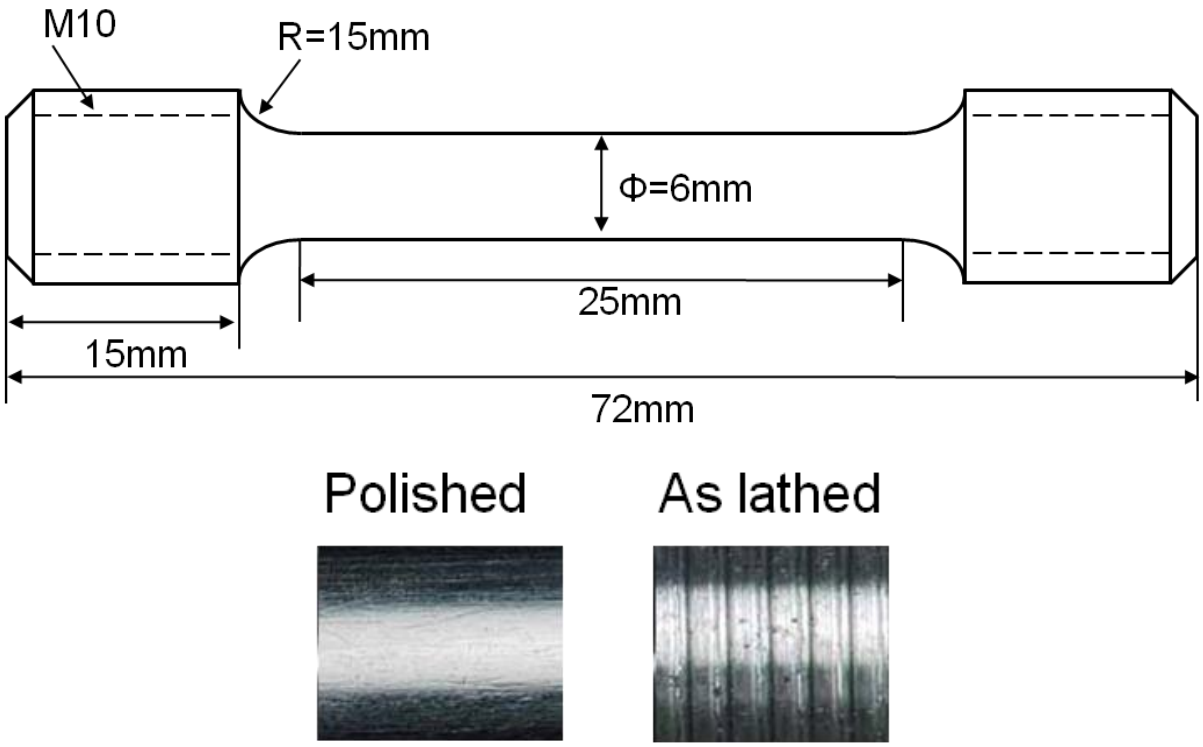

Fig. 1 the dimensions of sample for tensile test in hydrogen gas atmosphere and surface conditions of polished sample and as-lathed one.

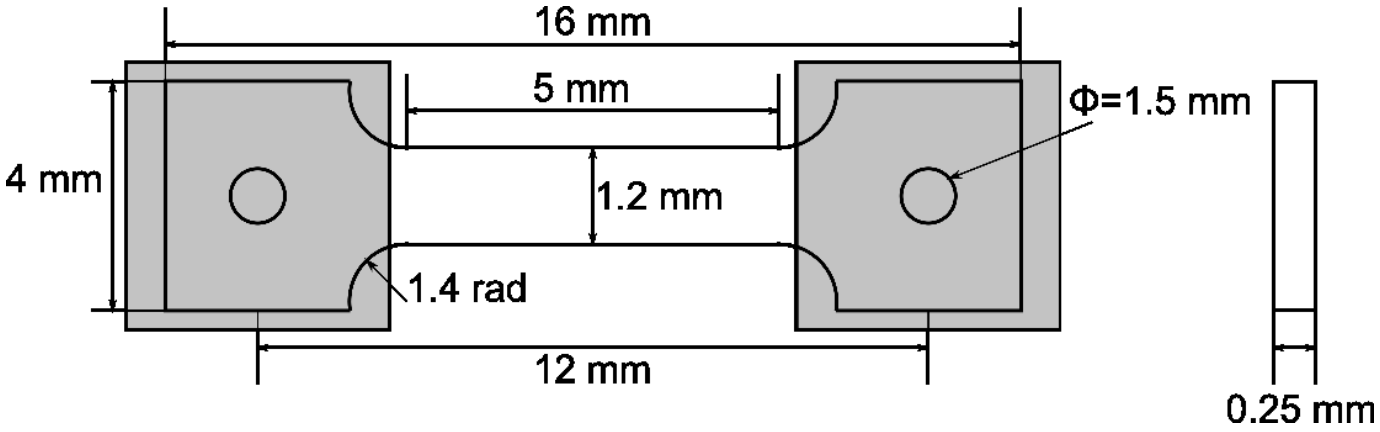

Fig.2 the dimensions of specimen for dynamic hydrogen tensile test.

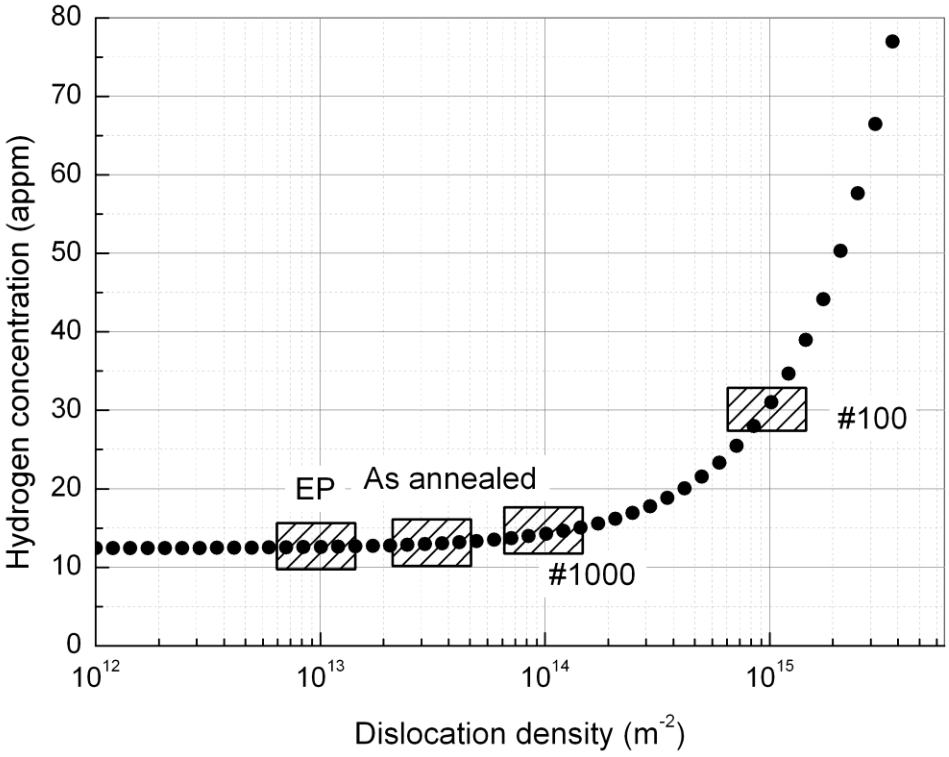

Fig. 3 the hydrogen concentration in the surface layers calculated as a function of dislocation density.

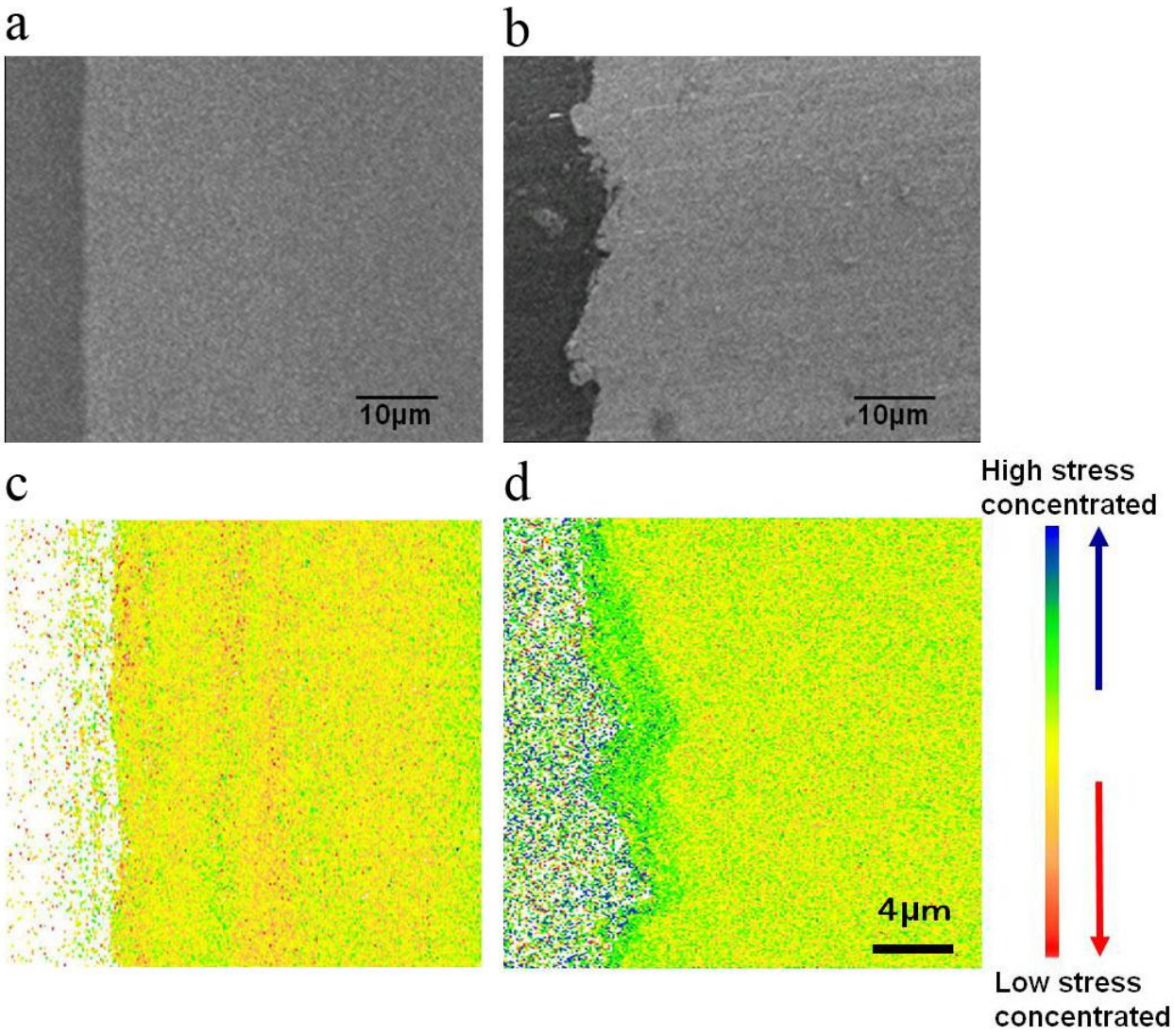

Fig. 4 the observation of surface structures of EP and #100 samples by SEM: (a) SEM microstructure of EP sample; (b) SEM microstructure of #100 samples; (c) EBSD figure of EP sample; (d) EBSD figure of #100 samples.

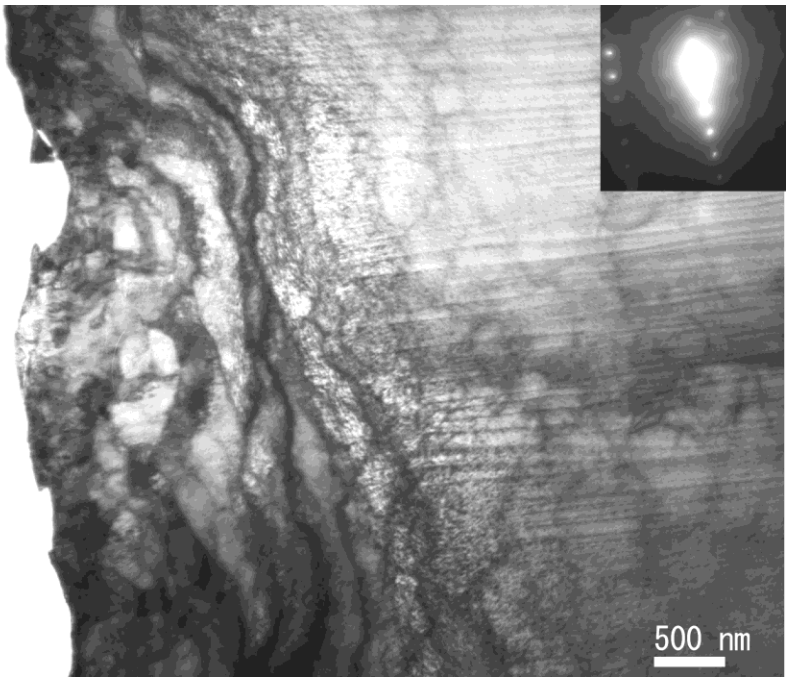

Fig. 5 the dislocation structure observed by TEM on the surface area of #100 samples.

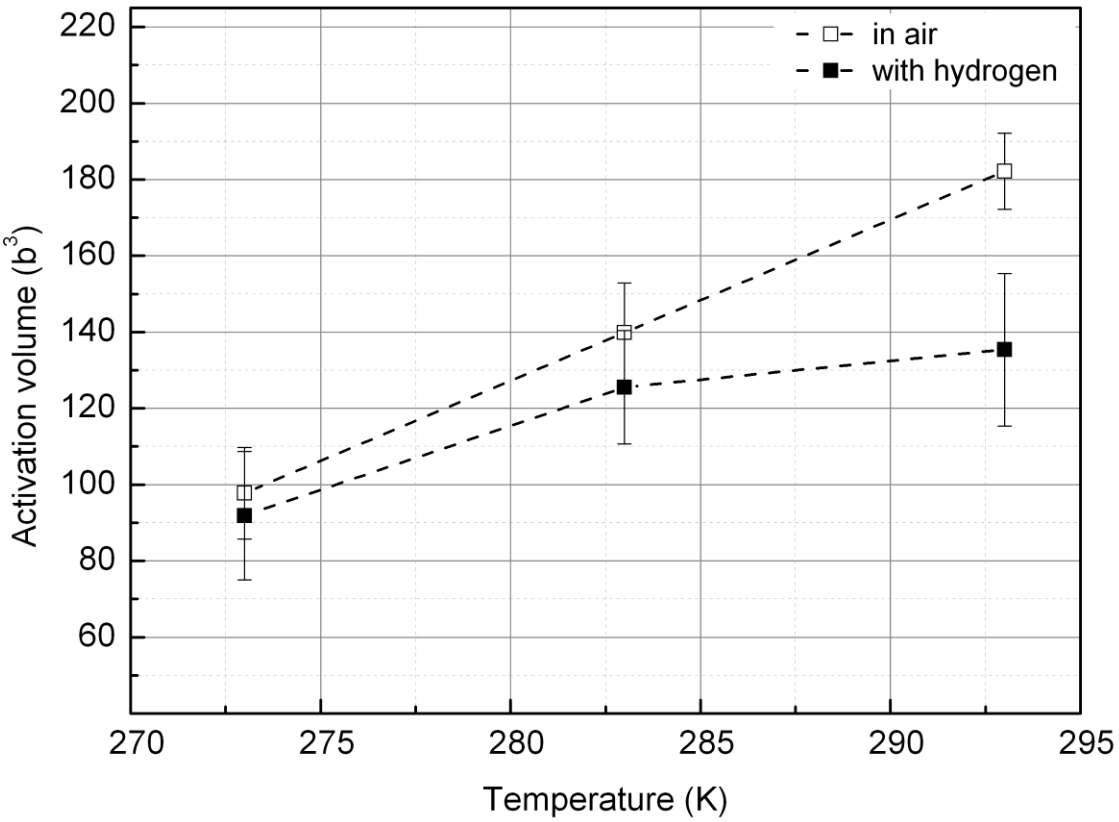

Fig. 6 the activation volume of EP samples measured from jump test in different temperature.

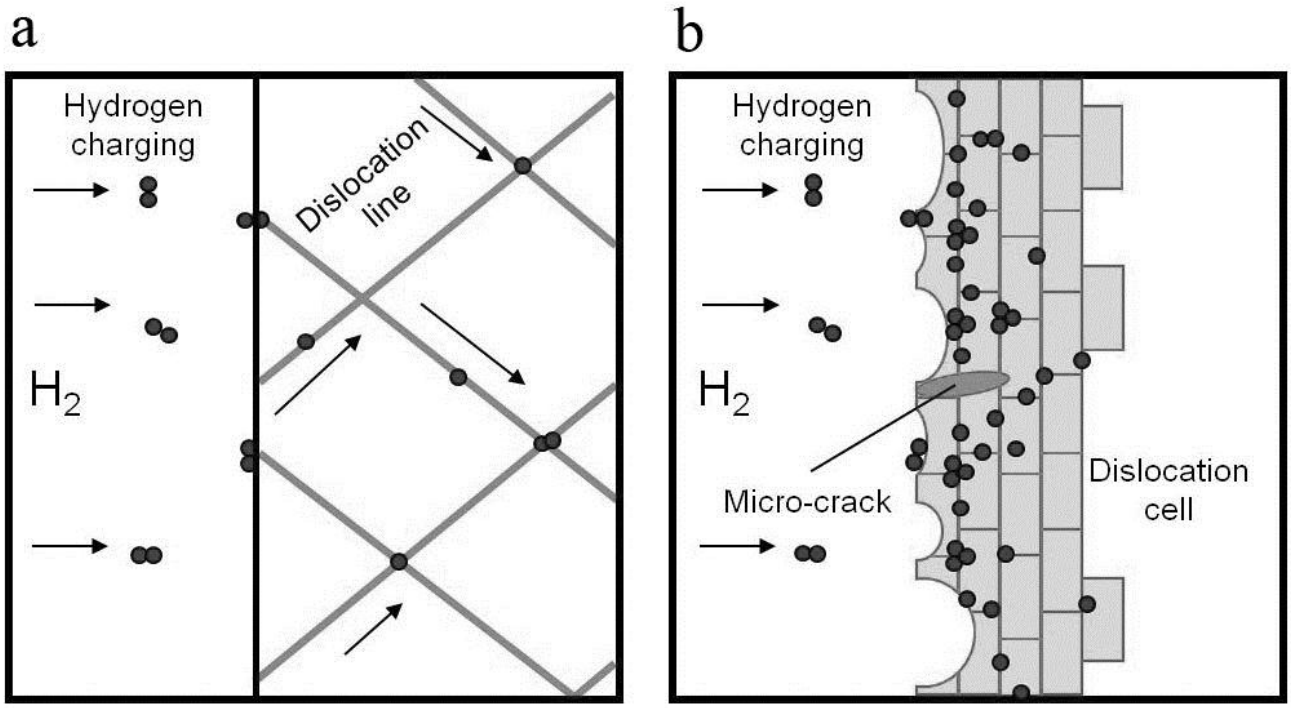

Fig. 7 the schematic diagram for possible hydrogen behavior at different surface structures.

Table 1 the composition of pure iron used in this study (wtppm).

Mg	Ca	Cr	Mn	Si	C	H	O	N	Fe
7	1	1	1	1	35	1.6	34	190	Balance

Table 2 the variation of tensile properties in rod specimen.

Sample		**Polished**			**As-lathed**	
Condition	**Air**	**H**	**Δ**	**Air**	**H**	**Δ**
YS (MPa)	163	146	-17	164	159	-5
UTS (MPa)	262	216	-46	267	230	-37
Elongation (%)	52	53	+1	57	44	-13

(Experimental error: ±5%)

Table 3 the summary of surface topography after tensile test in hydrogen gas environment.

		Surface	Fracture	RA%
In air	**As lathed**	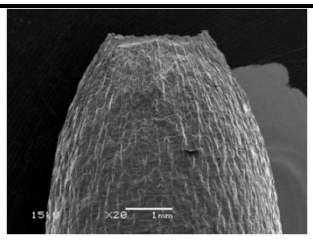	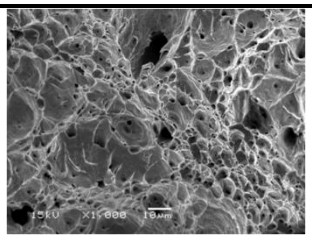	90
	Polished	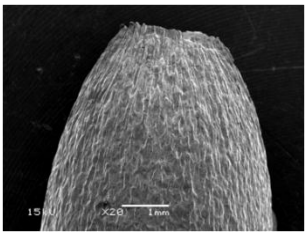	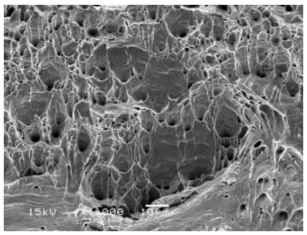	93
With hydrogen	**As lathed**	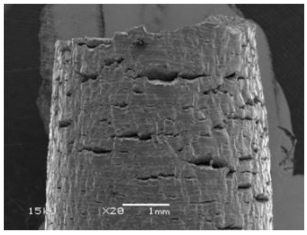	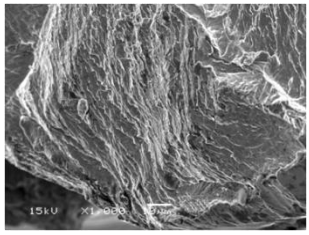	42
	Polished	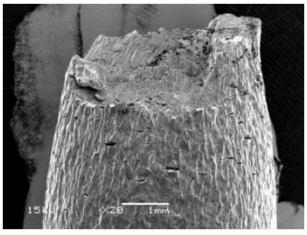	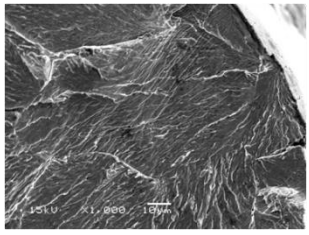	65

Table 4 the variation of tensile properties in small size specimen.

Sample	**EP**			**As-rolled**			**# 1000**			**# 100**		
Condition	**Air**	**H**	**Δ**	**Air**	**H**	**Δ**	**Air**	**H**	**Δ**	**Air**	**H**	**Δ**
YS (MPa)	110	96	-14	110	123	+13	138	132	-6	126	142	+16
UTS (MPa)	268	254	-14	271	287	+16	282	274	-8	281	310	+25
Elongation (%)	31	32	+1	30	26	-4	25	20	-5	22	19	-3

(Experimental error: ±4%)

Table 5 the summary of surface topography after tensile test in dynamic hydrogen charging condition.

		Surface	Fracture	RA%
In air	#100	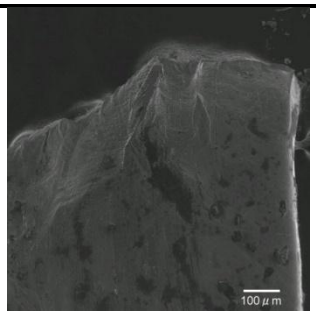	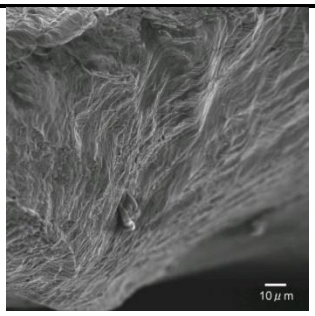	80
	EP	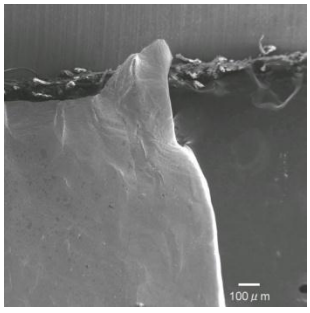	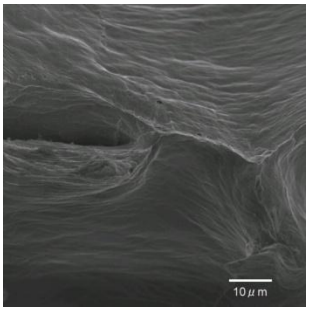	83
With hydrogen	#100	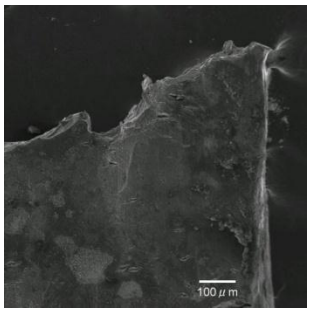	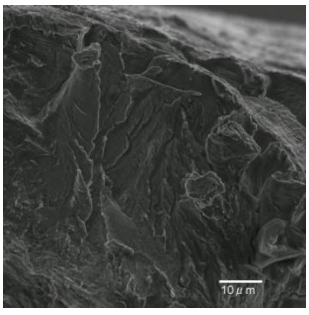	36
	EP	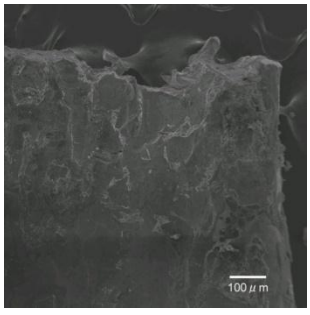	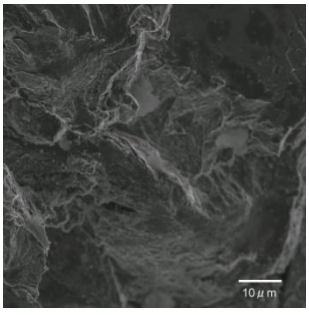	56